Optimal model reduction by time-domain moment matching for Lur'e-type models (extended version)

Fahim Shakib, Giordano Scarciotti, Marc Jungers, Alexander Yu Pogromsky, Alexey Pavlov, Nathan van de Wouw

Optimal model reduction by time-domain moment matching for Lur'e-type models (extended version)

Fahim Shakib, *Member, IEEE*, Giordano Scarciotti, *Senior Member, IEEE*, Marc Jungers, *Member, IEEE*, Alexander Yu Pogromsky, Alexey Pavlov, *Senior Member, IEEE*, and Nathan van de Wouw, *Fellow, IEEE*

***Abstract*— This paper considers the problem of model reduction for Lur'e-type models consisting of a feedback interconnection between linear dynamics and static nonlinearities. We propose an optimal variant of the time-domain moment-matching method in which the $\mathcal{H}_\infty$-norm of the error transfer-function matrix of the linear part of the model is minimised, while the static nonlinearities are inherited from the full-order model. We show that this approach also minimises an error bound on the $\mathcal{L}_2$-norm of the steady-state error between the responses of the full-order nonlinear model and the reduced-order nonlinear model. Furthermore, the proposed approach preserves both the Lur'e-type model structure as well as global stability properties. The problem is cast as an optimisation problem with bilinear matrix inequality constraints.This problem is then solved using a novel algorithm, although global convergence of the algorithm is not guaranteed.The effectiveness of the approach is illustrated in the reduction of a structural dynamics model of a linear beam with nonlinear supports.**

***Index Terms*— Model reduction, Moment matching, Global stability, Nonlinear feedback, Bilinear matrix inequalities, Coordinate-descent algorithm.**

I. Introduction

Model order reduction aims at finding reduced-order models that accurately describe the dynamical behaviour of full-order models [1], [2]. In this problem, it is a challenging task to find reduced-order models with optimal accuracy. For linear time-invariant (LTI) models, the optimal $\mathcal{H}_\infty$-reduction problem has been posed as an optimisation problem with bilinear matrix inequality (BMI) constraints [3]. Alternatively, optimal $\mathcal{H}_2$-reduction problems have pointed out necessary conditions for optimality and proposed sophisticated numerical algorithms, see [4] and references therein. Recently, [5] showed that the $\mathcal{H}_2$-problem can be solved globally, although its implementation is limited to small-scale models.

Fahim Shakib and Giordano Scarciotti are with the Department of Electrical and Electronic Engineering, Imperial College London, UK (email: {m.shakib,g.scarciotti}@imperial.ac.uk).

Marc Jungers is with the Université de Lorraine, CNRS, CRAN, F-54000 Nancy, France (email: marc.jungers@univ-lorraine.fr).

Alexander Yu Pogromsky and Nathan van de Wouw are with the Department of Mechanical Engineering, Eindhoven University of Technology, the Netherlands (email: {a.pogromsky,N.v.d.Wouw}@tue.nl).

Alexey Pavlov is with the Department of Geoscience and Petroleum, NTNU, Trondheim, Norway (email: alexey.pavlov@ntnu.no)

In the nonlinear case, it is difficult to characterise, let alone optimise, the error between the full-order model and the reduced-order model. For example, the moment matching approach [2] or the balancing approach [6] are *local* methods for which error bounds do not exist for generic inputs. Nonlinear reduction approaches with error bounds rely on the preservation of *global* model stability properties, see, e.g., [7]–[11] and references therein. However, these error bounds cannot be influenced in other ways than changing the order of the reduced-order model.Abstraction methods [12] also provide error bounds that are instrumental for guaranteeing the closed-loop performance of the full-order model for controllers designed based on the reduced-order model. However, these bounds have not been used for optimal model reduction.

This paper presents a moment-matching approach for the reduction of Lur'e-type models consisting of multivariable high-order LTI dynamics placed in feedback with a static multivariable nonlinear function, see Fig. 1. Lur'e-type models can capture physical systems (see [12], [13] and references therein) and also arise from system identification procedures [14] and nonlinear control designs [15]. The proposed reduction method preserves the Lur'e-type model structure by inheriting the nonlinear function from the full-order model and only reducing the order of the LTI dynamics to a user-defined and arbitrarily small order, see Fig. 1. First, we parameterise a set of reduced-order models using multivariable time-domain moment matching [16].We show that this set always contains at least one model that preserves the *global* input-to-state convergence (ISC) property [17], which is a strong form of model stability that guarantees the existence and uniqueness of steady-state responses. Preserving the ISC property is a prerequisite for deriving an error bound. Second, we search within this set for the model that (i) preserves the ISC property and (ii) minimises the error bound. The reduction problem is cast as an optimisation problem with BMI constraints, for which we propose a novel algorithm. This algorithm is of independent interest as it can be applied with minor adaptations to general optimisation problems with BMI constraints. Although the global convergence of the algorithm is not guaranteed,we show that the algorithm is effective in a case study based on an actuated beam with nonlinear supports. The numerical implementation of the BMI constraints currently limits the approach to models with up to hundreds of states.

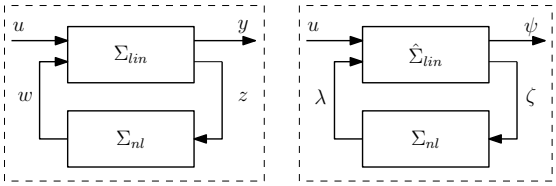

Fig. 1: Full-order (left) and reduced-order (right) Lur'e-type models, consisting of LTI dynamics placed in feedback with static nonlinearities. The order of the LTI dynamics is reduced.

The current paper (i) extends the single-input, single-output LTI approach in [18] to nonlinear multiple-input, multiple-output (MIMO) Lur'e-type models, (ii) derives and minimises an error bound between responses of the full-order and reduced-order nonlinear models, (iii) derives conditions for preserving the convergence stability property, (iv) provides an existence result for a convergence-preserving reduced-order model for any reduction order, (v) provides a completeness result for the set of reduced-order nonlinear models, and (vi) presents a numerical case study based on a nonlinear structural dynamics model. Furthermore, the current approach has several advantages over the recently published method [13], namely: (i) it uses a recently developed MIMO version of LTI moment matching [16] to achieve a more efficient reduction; and (ii) it directly minimises the error bound on the responses of the nonlinear model as opposed to a proxy for it.

The remainder of this paper is structured as follows. Section II proposes a model order reduction approach for Lur'e-type models. Section III presents an algorithm for solving this problem. Section IV describes the results of two numerical case studies. Section V gives the concluding remarks. This paper is an extended author version of a brief paper in press for publication in the Transaction of Automatic Control (TAC) journal with title 'Optimal model reduction by time-domain moment matching for Lur'e-type models'. This extended version includes the proofs of all the results, some of which were omitted from the TAC paper for reasons of space. All proofs in this extended version were made available to the TAC review process.

Notation: The symbols $\mathbb{R}, \mathbb{C}, \mathbb{C}^0, \mathbb{C}^-$, and $\mathbb{N}$ denote the set of real numbers, complex numbers, complex numbers with zero real parts, complex numbers with negative real parts, and natural numbers (excluding 0), respectively. The symbols I_n and 0_n denote the $n \times n$ identity and zero matrices, respectively, and $0_{n\times\nu}$ denotes the zero matrix of dimensions $n \times \nu$. For $A \in \mathbb{R}^{n\times n}$, $\sigma(A)$ denotes its spectrum and $A^\top$ denotes its transpose. For a symmetric matrix $A \in \mathbb{R}^{n\times n}$, $A \succ 0$ ($A \prec 0$) denotes that A is positive (negative) definite. In symmetric block matrices, the element $\star$ is induced by transposition. For matrices $\mathcal{X}, A \in \mathbb{R}^{n\times n}, \mathcal{B} \in \mathbb{R}^{n\times m}, \mathcal{C} \in \mathbb{R}^{p\times n}$, and the constant $\gamma \geq 0$, we use the short-hand notations

$$\mathrm{He}\,(A) \coloneqq A + A^\top, \tag{1a}$$

$$\mathcal{N}_\gamma(\mathcal{A},\mathcal{B},\mathcal{C},\mathcal{X}) \coloneqq \begin{bmatrix} \mathrm{He}\,(\mathcal{X}\mathcal{A}) & \mathcal{X}\mathcal{B} & \mathcal{C}^\top \\ \star & -\gamma I_m & 0_{m\times p} \\ \star & \star & -\gamma I_p \end{bmatrix}. \tag{1b}$$

For $\gamma = 1$, we write $\mathcal{N}$ instead of $\mathcal{N}_1$. For a vector x, its Euclidean norm is denoted by $|x|$. For a piecewise-continuous T-periodic signal x defined on $\mathbb{R}$, the $\mathcal{L}_2$-norm is denoted and defined by $\|x\|_2^2 \coloneqq \frac{1}{T}\int_0^T |x(t)|^2 \mathrm{d}t$. The symbol $\mathcal{L}_2^m(T)$ denotes the class of T-periodic piecewise-continuous functions $u : \mathbb{R} \to \mathbb{R}^m$ satisfying $\|u\|_2 < +\infty$, whereas $\mathcal{L}_\infty^m$ denotes the class of essentially-bounded piecewise-continuous functions $u : \mathbb{R} \to \mathbb{R}^m$. For a transfer-function matrix Φ defined on $\mathbb{C}$, with all its poles in $\mathbb{C}^-$, its $\mathcal{H}_\infty$-norm is defined by $\|\Phi\|_{\mathcal{H}_\infty} \coloneqq \sup_{\omega\in[0,\infty)} \bar{\rho}(\Phi(j\omega))$ with $\bar{\rho}$ the maximum singular value of Φ and $j \coloneqq \sqrt{-1}$.

II. Optimal moment matching for multivariable Lur'e-type models

This section presents a moment-matching approach for the order reduction of the Lur'e-type models depicted in Fig. 1. First, in Section II-A, preliminaries on moments for Lur'e-type models are recalled. Then, in Section II-B, the considered reduction problem is formalised. Finally, in Section II-C, we cast this problem into an equivalent, tractable problem, which we solve by an algorithm presented in Section III.

A. Moments of convergent Lur'e-type models

Consider Lur'e-type models described by:

$$\Sigma_{lin}: \quad \begin{cases} \dot{x} &= Ax + B_u u + B_w w, \\ y &= C_y x, \\ z &= C_z x, \end{cases} \tag{2a}$$

$$\Sigma_{nl}: \quad \{ \; w = \varphi(z), \tag{2b}$$

where $x(t) \in \mathbb{R}^n$ is the state, $u(t) \in \mathbb{R}^m$ is the input, $y(t) \in \mathbb{R}^p$ is the output, $z(t) \in \mathbb{R}^q$ is the input to the nonlinear block, and $w(t) \in \mathbb{R}^q$ is the output of the nonlinear block. The model matrices are $A \in \mathbb{R}^{n\times n}, B_u \in \mathbb{R}^{n\times m}, B_w \in \mathbb{R}^{n\times q}, C_y \in \mathbb{R}^{p\times n}$, and $C_z \in \mathbb{R}^{q\times n}$. We define $B \coloneqq \begin{bmatrix} B_u & B_w \end{bmatrix}$ and $C^\top \coloneqq \begin{bmatrix} C_y^\top & C_z^\top \end{bmatrix}$. The nonlinear block Σ_{nl} is a decentralised nonlinear function $\varphi : \mathbb{R}^q \to \mathbb{R}^q$, such that each element $\varphi_{(i)}, i \in \{1,\ldots,q\}$, is only a function of the i-th input $z_{(i)}$ and satisfies both $\varphi_{(i)}(0) = 0$ and the incremental sector condition

$$|\varphi_{(i)}(z_{(i)}^a) - \varphi(z_{(i)}^b)| \leq |z_{(i)}^a - z_{(i)}^b|, \quad \forall\, z_{(i)}^a, z_{(i)}^b \in \mathbb{R}. \tag{3}$$

Models (2) with globally Lipschitz nonlinearities can be transformed so that (3) is satisfied, see [19]. Fig. 1 depicts model (2) schematically.

Consider the signal generator

$$\dot{\tau} = S\tau, \quad u = L\tau, \tag{4}$$

where $\tau(t) \in \mathbb{R}^\nu, u(t) \in \mathbb{R}^m$, and the pair $(S \in \mathbb{R}^{\nu\times\nu}, L \in \mathbb{R}^{m\times\nu})$ is observable. A *global* definition of moments of the model (2) is recalled next from [13].

Definition 1 ([13]): Consider model (2) with u generated by (4) with (S, L) observable. Suppose there exists a unique function $\pi : \mathbb{R}^\nu \to \mathbb{R}^n : \tau \mapsto \pi(\tau)$, such that the graph

$$\mathcal{M} \coloneqq \{(\tau, x) : x = \pi(\tau), \tau \in \mathbb{R}^\nu\} \tag{5}$$

is invariant. Then, the function $C_y\pi$ is called the moment of the model (2) at (S, L).

A *global* form of model stability is required to ensure the existence and uniqueness of π. We recall the notions of *global uniform convergence* and *input-to-state convergence* (ISC).

Definition 2 ([17]): The model (2) is said to be globally uniformly convergent if for every input $u \in \mathcal{L}_\infty^m$, there exists a solution $\bar{x}_u$ to (2) that satisfies the following conditions:

- $\bar{x}_u$ is defined and bounded on $\mathbb{R}$,
- $\bar{x}_u$ is globally uniformly asymptotically stable.

The solution $\bar{x}_u$ is called the *steady-state* solution.

Definition 3 ([17]): The model (2) is said to be input-to-state convergent if it is globally uniformly convergent and, for every input $u \in \mathcal{L}_\infty^m$, model (2) is input-to-state stable with respect to the steady-state solution $\bar{x}_u$.

Sufficient conditions for the global uniform convergence and the ISC property of the model (2) are presented next.

Theorem 1: Consider the model (2). Suppose that

- the matrix A is Hurwitz, i.e., $\sigma(A) \subset \mathbb{C}^-$.
- the decentralised nonlinearity φ satisfies $\varphi(0) = 0$ and the incremental sector condition (3).
- the gain condition

$$\left\|\Phi_{(z,w)}\right\|_{\mathcal{H}_\infty} =: \gamma_{zw} < 1 \tag{6}$$

is satisfied, where $\Phi_{(z,w)}(s) \coloneqq C_z(sI-A)^{-1}B_w$, $s \in \mathbb{C}$.

Then, the model (2) is globally uniformly convergent and input-to-state convergent for the class of inputs $\mathcal{L}_\infty^m$. □

Proof: The proof can be found in Appendix I. ■

To streamline the presentation, we summarise the required assumptions.

Assumption 1: Model (2) satisfies all the conditions of Theorem 1. The pair (S, L) in (4) is observable and the eigenvalues of S are simple and located on the imaginary axis.

Under Assumption 1, the mapping π in (5) exists and is unique, see [13, Lemma 5]. Furthermore, the steady-state solution $\bar{x}_u$ of the model (2) satisfies $\bar{x}_u = \pi(\tau)$, where τ is the state of the signal generator (4).

B. The optimal nonlinear moment-matching problem

As an approximation to (2), consider the Lur'e-type model

$$\hat{\Sigma}_{lin}: \quad \begin{cases} \dot{\xi} &= F\xi + G_u u + G_\lambda \lambda, \\ \psi &= H_\psi \xi, \\ \zeta &= H_\zeta \xi, \end{cases} \tag{7a}$$

$$\Sigma_{nl}: \quad \{ \ \lambda = \varphi(\zeta), \tag{7b}$$

where $\xi(t) \in \mathbb{R}^\nu$, $u(t) \in \mathbb{R}^m$, $\psi(t) \in \mathbb{R}^p$, $\zeta(t) \in \mathbb{R}^q$, $\lambda(t) \in \mathbb{R}^q$, $F \in \mathbb{R}^{\nu\times\nu}, G_u \in \mathbb{R}^{\nu\times m}, G_\lambda \in \mathbb{R}^{\nu\times q}, H_\psi \in \mathbb{R}^{p\times\nu}$, and $H_\zeta \in \mathbb{R}^{q\times\nu}$. We define $G \coloneqq \begin{bmatrix} G_u & G_\lambda \end{bmatrix}$ and $H^\top \coloneqq \begin{bmatrix} H_\psi^\top & H_\zeta^\top \end{bmatrix}$. The model (7) inherits the nonlinear block Σ_{nl} of (2) and thus preserves the Lur'e-type structure, see Fig. 1. The transfer functions associated with (7a) are

$$\Gamma_{(i,k)}(s) \coloneqq H_i(sI - F)^{-1}G_k, \quad s \in \mathbb{C}, \tag{8}$$

for $i \in \{\psi, \zeta\}$, $k \in \{u, \lambda\}$ and, for $\sigma(F) \subset \mathbb{C}^-$, the following corresponding gains are defined as:

$$\gamma_{ik} \coloneqq \left\|\Gamma_{(i,k)}\right\|_{\mathcal{H}_\infty} < +\infty, \ i \in \{\psi, \zeta\}, \ k \in \{u, \lambda\}. \tag{9}$$

The collection of transfer-function matrices is defined as:

$$\Gamma(s) \coloneqq \begin{bmatrix} \Gamma_{(\psi,u)}(s) & \Gamma_{(\psi,\lambda)}(s) \\ \Gamma_{(\zeta,u)}(s) & \Gamma_{(\zeta,\lambda)}(s) \end{bmatrix}, \quad s \in \mathbb{C}. \tag{10}$$

Similarly, the transfer-function matrices associated with the LTI part of the full-order model (2) are denoted by Φ and $\Phi_{(i,k)}$, for $i \in \{y, z\}, k \in \{u, w\}$, and are defined similarly to Γ in (10) and $\Gamma_{(i,k)}$ in (8), respectively. Similar to (9), we define the gains $\gamma_{ik}, i \in \{y, z\}, k \in \{u, w\}$.

By Assumption 1, $\sigma(A) \subset \mathbb{C}^-$. The proposed reduction approach ensures that the reduced-order model (7) satisfies the conditions of Theorem 1, resulting in $\sigma(F) \subset \mathbb{C}^-$. Then, there exists a $0 \leq \gamma < +\infty$ such that:

$$\|\Phi - \Gamma\|_{\mathcal{H}_\infty} \leq \gamma. \tag{11}$$

Although γ characterises an error bound on LTI transfer-function matrices, we show that it also plays a central role in the error between the responses of the Lur'e-type models.

Lemma 1: Consider models (2) and (7) and suppose that both satisfy the conditions of Theorem 1. Then, for any $u \in \mathcal{L}_2^m(T)$, the steady-state output error $\bar{y}_u - \bar{\psi}_u$ is bounded by

$$\left\|\bar{y}_u - \bar{\psi}_u\right\|_2 \leq \gamma \left(1 + \frac{\gamma_{yw}}{1 - \gamma_{zw}}\right)\left(1 + \frac{\gamma_{\zeta u}}{1 - \gamma_{\zeta\lambda}}\right)\|u\|_2 \tag{12}$$

with γ defined in (11), the constants $\gamma_{\zeta u}$ and $\gamma_{\zeta\lambda}$ defined in (9), and γ_{yw} and γ_{zw} defined similarly. □

Proof: The proof can be found in Appendix II. ■

Let $H_\psi\theta$ be the moment of the reduced-order model (7), where θ plays the role of π in Definition 1. Then, noting that $\bar{x}_u = \pi(\tau)$ and $\bar{\xi}_u = \theta(\tau)$, we observe that (12) also bounds the mismatch in moment $C_y\pi(\tau) - H_\psi\theta(\tau)$.

Model reduction by moment matching aims to find reduced-order models that share the *same* moment as the full-order model [2], i.e., match $H_\psi\theta$ to $C_y\pi$. However, achieving moment matching in the structure-preserving setting faces two challenges. First, because Σ_{nl} generates an infinite number of harmonics, moment matching generally requires an infinite number of interpolation points, i.e., $\nu = \infty$, see [13]. Second, finding an analytical expression for the mapping π in Definition 1 is challenging, or even infeasible. Therefore, the proposed method in this paper aims to achieve *linear* moment matching between the LTI parts of the Lur'e-type models. In addition, it exploits the parametric freedom of moment matching to ensure ISC preservation and to minimise the error bound in Lemma 1, thus ensuring an accurate *approximation* between the moments $C_y\pi$ and $H_\psi\theta$.

The moment of Σ_{lin} in (2a) at (S, L) is $C\Pi$ [2], where $\Pi \in \mathbb{R}^{n\times\nu}$ is the solution of the Sylvester equation

$$\Pi S = A\Pi + BL. \tag{13}$$

Analogously, the moment of $\hat{\Sigma}_{lin}$ in (7a) is $H\Theta$, where Θ plays the role of Π. The linear model $\hat{\Sigma}_{lin}$ in (7a) achieves moment matching at (S, L) if $H\Theta = C\Pi$. The reduction problem for Lur'e-type models is formally presented next.

Problem 1: Consider the full-order model (2) and a given pair (S, L) in (4). Suppose Assumption 1 holds. Consider the reduced-order model (7). The problem of *Optimal $\mathcal{H}_\infty$-model reduction by approximate moment matching* consists in

solving the following constrained optimisation problem:

$$\begin{aligned} \min_{F,G_u,G_\lambda,H_\zeta,H_\psi,\gamma} \quad & \gamma && \text{(14a)}\\ \text{subject to} \quad & \|\Phi-\Gamma\|_\infty < \gamma, && \text{(14b)}\\ & \left\|\Gamma_{(\zeta,\lambda)}\right\|_\infty < 1, && \text{(14c)}\\ & C\Pi = H\Theta. && \text{(14d)} \end{aligned}$$

Problem 1 minimises γ, which plays a prominent role in the error bound in Lemma 1. Constraint (14c) guarantees the satisfaction of condition (6) in Theorem 1 (written for model (7)), which leads to the preservation of ISC. Constraint (14d) guarantees LTI moment matching and provides a frequency-domain interpretation of the reduction method [16].

Remark 1: The interpolation points $\sigma(S)$ can be chosen as the zero frequency, resonance frequencies, and other frequencies of interest. The selection of tangential directions in the matrix L is less intuitive and we refer to [16] for more details on the relation between tangential directions and moments.

C. An equivalent, tractable, and solvable problem

The set of models that satisfy (14d) is given in the following theorem. Hereto, given a S and L, the set $\mathcal{G}_M$ is defined as

$$\mathcal{G}_M := \left\{ G \in \mathbb{R}^{\nu\times(m+q)} \,:\, \sigma(S)\cap\sigma(S-GL)=\emptyset \right\}. \quad (15)$$

Theorem 2 ([16]): Consider the full-order model (2a) and the observable pair (S,L) in (4). Suppose $\sigma(S)\cap\sigma(A)=\emptyset$. Then, for any $G\in\mathcal{G}_M$, model (7a) with matrices

$$F := S-GL, \quad H := C\Pi, \quad (16)$$

where $\Pi\in\mathbb{R}^{n\times\nu}$ is the unique solution to (13) achieves moment matching at (S,L). □

The set $\mathcal{G}_M$ is parameterised by the matrix G. It contains all models that satisfy constraint (14d) as stated in the next lemma. This is a MIMO extension of [2, Proposition 1].

Lemma 2: Consider any ν-th-order model described by

$$\dot{\hat{\xi}} = \hat{F}\hat{\xi} + \hat{G}_u u + \hat{G}_\lambda \lambda, \quad \hat{\psi} = \hat{H}_\psi \hat{\xi}, \quad \hat{\zeta} = \hat{H}_\zeta \hat{\xi}, \quad (17)$$

that satisfies the constraint (14d), i.e., admits a unique full-rank solution $\hat{\Theta}\in\mathbb{R}^{\nu\times\nu}$ to

$$\hat{F}\hat{\Theta} + \hat{G}L = \hat{\Theta}S, \quad C\Pi = \hat{H}\hat{\Theta}, \quad (18)$$

where $\hat{G} := \begin{bmatrix}\hat{G}_u & \hat{G}_\lambda\end{bmatrix}$, $\hat{H}^\top := \begin{bmatrix}\hat{H}_\psi^\top & \hat{H}_\zeta^\top\end{bmatrix}$. Model (7a) with (F,H) in (16) and $G=\hat{\Theta}^{-1}\hat{G}\in\mathcal{G}_M$ is equivalent to (17) under the similarity transformation $\hat{\xi}=\hat{\Theta}\xi$. □

Proof: The proof can be found in Appendix III. ■

Next, we exploit the freedom in the matrix G in $\mathcal{G}_M$ to parameterise a subset of $\mathcal{G}_M$ that satisfies the constraints (14b) and (14c) for a fixed $\gamma>0$.

Consider the LTI error dynamics:

$$\begin{aligned} \begin{bmatrix}\dot{x}\\ \dot{\xi}\end{bmatrix} &= \underbrace{\begin{bmatrix}A & 0_{n\times\nu}\\ 0_{\nu\times n} & S-GL\end{bmatrix}}_{\mathcal{A}}\begin{bmatrix}x\\ \xi\end{bmatrix} + \underbrace{\begin{bmatrix}B_u & B_w\\ G_u & G_\lambda\end{bmatrix}}_{\mathcal{B}}\begin{bmatrix}u & w\end{bmatrix}\\ \begin{bmatrix}e_y\\ e_z\end{bmatrix} &= \underbrace{\begin{bmatrix}C_y & -H_\psi\\ C_z & -H_\zeta\end{bmatrix}}_{\mathcal{C}}\begin{bmatrix}x\\ \xi\end{bmatrix}, \end{aligned} \quad (19)$$

and the set of models

$$\begin{aligned} \mathcal{G}_\gamma := \{ G\in\mathbb{R}^{\nu\times(m+q)} : \exists \mathcal{X}_1 \succ 0_{n+\nu}, \exists \mathcal{X}_2 \succ 0_\nu : \\ \mathcal{N}_\gamma(\mathcal{A},\mathcal{B},\mathcal{C},\mathcal{X}_1) \prec 0_{n+\nu+m+p+2q}, \\ \mathcal{N}(S-GL, G_\lambda, H_\zeta, \mathcal{X}_2) \prec 0_{\nu+2q}\}, \end{aligned} \quad (20)$$

where $\mathcal{N}_\gamma$ and $\mathcal{N}$ are defined in (1b), $\mathcal{A},\mathcal{B},\mathcal{C}$ are defined in (19), H_ζ is defined in Theorem 2, and G_λ is a submatrix of G. The satisfaction of the constraints in (20) ensures the satisfaction of (14b) and (14c), where the latter guarantees ISC preservation for the reduced-order Lur'e-type model (7). We first show that, regardless of the order ν of the reduced model, the set $\mathcal{G}_\gamma$ is non-empty for some $\gamma<\infty$. This is a stronger result than the results in [8], [10], [11], where the reduction order ν must be sufficiently large to preserve model stability.

Lemma 3: Consider the full-order model (2) and the reduced-order model (7). Suppose Assumption 1 holds. Then, there exists a $0\le\gamma^{[0]}<+\infty$ and $G^{[0]}\in\mathbb{R}^{\nu\times(m+q)}$ such that $G^{[0]}\in\mathcal{G}_{\gamma^{[0]}}$ with $\mathcal{G}_\gamma$ in (20). Furthermore, such a $G^{[0]}$ is given by $G^{[0]}=\mathcal{X}^{-1}\begin{bmatrix}Q_1 & Q_2\end{bmatrix}$, where $\mathcal{X}\succ 0_\nu$, $Q_1\in\mathbb{R}^{\nu\times m}$, and $Q_2\in\mathbb{R}^{\nu\times q}$ are such that the linear matrix inequalities

$$\mathcal{N}(\mathcal{X}S - \begin{bmatrix}Q_1 & Q_2\end{bmatrix}L, Q_2, H_\zeta, I_\nu) \prec 0. \quad (21)$$

are satisfied. The corresponding $\gamma^{[0]}$ is given by $\gamma^{[0]} = \|\Psi-\Gamma\|_{\mathcal{H}_\infty} < +\infty$. □

Proof: The proof can be found in Appendix IV. ■

We are now ready to present the main result of this paper.

Theorem 3: Consider the full-order model (2) and the signal generator (4). Suppose Assumption 1 holds. Then, the following statements are true for any order $\nu\in\mathbb{N}$:

1) The set of all reduced-order models (7) satisfying constraints (14b)–(14d) of Problem 1 is characterised, up to a similarity transformation, by (F,H) defined by (16) with $G\in\mathcal{G}_\gamma\subset\mathcal{G}_M$.
2) The set $\mathcal{G}_\gamma$ is non-empty for some $0\le\gamma<+\infty$. In addition, if the LTI part (2a) of the full-order model is balanced with Hankel singular values $\bar{h}_1\ge\ldots\ge\bar{h}_\nu\ge\bar{h}_{\nu+1}\ge\ldots\ge\bar{h}_n$, then the set $\mathcal{G}_\gamma$ is empty for $\gamma<\bar{h}_{\nu+1}$.
3) For any model (7) satisfying (14b)–(14d), the difference between the steady-state outputs of (2) and (7) corresponding to an input $u\in\mathcal{L}_2^m(T)$, is bounded by (12).

□

Proof: The proof can be found in Appendix V. ■

Consequently, the optimisation problem in Problem 1 is replaced by the equivalent problem

$$\begin{aligned} \min_{G,\gamma} \quad & \gamma \\ \text{subject to } & G\in\mathcal{G}_\gamma. \end{aligned} \quad (22)$$

Compared to (14), optimisation problem (22) contains only $\nu\times(m+q)$ model parameters. Note that the set $\mathcal{G}_\gamma$ contains all models that satisfy the constraints of Problem 1, up to a similarity transformation.In addition, regardless of the order ν, the set $\mathcal{G}_\gamma$ is not empty for some, possibly large, γ.

III. Algorithm for solving the optimal model reduction problem

This section presents a coordinate-descent algorithm (CDA) [20] for solving the optimisation problem (22) subject to BMI constraints. The proposed iterative algorithm combines two CDAs and allows switching if either CDA becomes stuck.

A. Primal and Finsler's form constraints

The set $\mathcal{G}_\gamma$ in (20) is characterised by bilinear matrix inequality constraints in the matrix variable G and positive definite matrices $\mathcal{X}_1$ and $\mathcal{X}_2$, the latter collected in $\mathcal{X} := \{\mathcal{X}_1, \mathcal{X}_2\}$. These constraints can be written in a standard (*primal*) form $\mathcal{R}_p(\mathcal{X}, G, \gamma) \prec 0$, where

$$\mathcal{R}_p(\mathcal{X}, G, \gamma) := \mathcal{M}_1(\mathcal{X}, \gamma) + \mathrm{He}\left(\mathcal{M}_2(\mathcal{X})\mathcal{M}_3^\top(G)\right), \quad (23)$$

and

$$\begin{aligned}
\mathcal{M}_1(\mathcal{X}, \gamma) :=& \text{blkdiag}\left(-\mathcal{X}_1, -\mathcal{X}_2, \bar{\mathcal{N}}_\gamma, \tilde{\mathcal{N}}\right),\\
\bar{\mathcal{N}}_\gamma :=& \mathcal{N}_\gamma\left(\begin{bmatrix} A & 0_{n\times\nu} \\ 0_{\nu\times n} & S \end{bmatrix}, \begin{bmatrix} B \\ 0_{\nu\times(m+q)} \end{bmatrix}, \mathcal{C}, \mathcal{X}_1\right),\\
\tilde{\mathcal{N}} :=& \mathcal{N}\left(S, 0_{\nu\times q}, H_\zeta, \mathcal{X}_2\right),\\
\mathcal{M}_2(\mathcal{X}) :=& \text{blkdiag}\left(0_{n+2\nu}, \begin{bmatrix} \mathcal{X}_1 \\ 0_{(m+q)\times(n+\nu)} \end{bmatrix}, \begin{bmatrix} \mathcal{X}_2 \\ 0_{q\times\nu} \\ 0_{q\times\nu} \end{bmatrix}\right),\\
\mathcal{M}_3(G) :=& \text{blkdiag}\left(0_{n+2\nu}, \bar{G}^\top, \begin{bmatrix} -(GL)^\top \\ G_\lambda^\top \\ 0_{q\times\nu} \end{bmatrix}\right),\\
\bar{G} :=& \begin{bmatrix} 0_n & 0_{n\times\nu} & 0_{n\times(m+q)} & 0_{n\times(p+q)} \\ 0_{\nu\times n} & -GL & G & 0_{\nu\times(p+q)} \end{bmatrix}.
\end{aligned}$$

Note that $\mathcal{M}_1, \mathcal{M}_2$, and $\mathcal{M}_3$ are *linear* in their arguments, and products between $\mathcal{X}$ and G in (23) only arise from products between $\mathcal{M}_2$ and $\mathcal{M}_3$. The square matrix $\mathcal{R}_p$ has $2n + 4\nu + 4q + m + p$ rows.

Thanks to the Finsler's Lemma [21], the constraint in the primal form $\mathcal{R}_p(\mathcal{X}, G, \gamma) \prec 0$ can be rewritten in the so-called *Finsler's form*: $\mathcal{R}_F(\mathcal{X}, N, G, \gamma) \prec 0$ with $N \in \mathbb{R}^{(2n+4\nu)\times(4n+8\nu+4q+m+p)}$ an additional decision variable. The matrix $\mathcal{R}_F$ is as follows:

$$\mathcal{R}_F(\mathcal{X}, N, G, \gamma) := \mathcal{M}(\mathcal{X}, \gamma) + \mathrm{He}\left(\begin{bmatrix} \mathcal{M}_3(G) \\ -I_{2n+4\nu} \end{bmatrix} N^\top\right), \quad (24)$$

where

$$\mathcal{M}(\mathcal{X}, \gamma) := \begin{bmatrix} \mathcal{M}_1(\mathcal{X}, \gamma) & \mathcal{M}_2(\mathcal{X}) \\ \star & 0_{2n+4\nu} \end{bmatrix}. \quad (25)$$

The matrix $\mathcal{R}_F(\mathcal{X}, N, G, \gamma)$ contains no products between $\mathcal{X}$ and G, but instead contains a product between G and N. By Finsler's Lemma [21], the constraints are equivalent in primal and Finsler's form, i.e., for given $\mathcal{X}, G, \gamma$, the inequality $\mathcal{R}_p(\mathcal{X}, G, \gamma) \prec 0$ holds if and only if there exists an additional matrix N such that $\mathcal{R}_F(\mathcal{X}, N, G, \gamma) \prec 0$. The square matrix $\mathcal{R}_F$ has $4n + 8\nu + 4q + m + p$ rows.

B. Combination of CDAs

The CDA is listed in Algorithm 1 for both the primal and the Finsler's forms. In Step 3, for a given, fixed G, the optimisation problem with LMI constraints in $\mathcal{X}$ in primal form or $\mathcal{X}$ and N in Finsler's form is solved for $\mathcal{X}$ and γ, or respectively $\mathcal{X}, N$, and γ. The $\mathcal{X}$, respectively N, computed in Step 3 is fixed in Step 4 and the optimisation problem with LMI constraints in G is solved for G and γ, or respectively $\mathcal{X}, G$, and γ. The CDAs can be initialised using Lemma 3.

Algorithm 1 CDA for constraints in primal or Finsler's form

Input: Constraints $\mathcal{R}_p \prec 0$ in (23) in primal form or $\mathcal{R}_F \prec 0$ in (24) in Finsler's form, any $\gamma^{[0]} > 0$ and matrix $G^{[0]} \in \mathcal{G}_{\gamma^{[0]}}$, and accuracy threshold $\epsilon > 0$.

1: Set iteration index $i = 1$.
2: **while** $(\gamma^{[i-1]} - \gamma^{[i]})/\gamma^{[i]} \geq \epsilon$ **do**
3: Solve the optimisation problem
Switch form **do**
case primal
$$\left(\mathcal{X}^{[i]}, \cdot\right) = \arg\min_{\mathcal{X},\gamma} \gamma \text{ subject to } \mathcal{R}_p(\mathcal{X}, G^{[i-1]}, \gamma) \prec 0.$$
case Finsler's
$$\left(\cdot, N^{[i]}, \cdot\right) = \arg\min_{\mathcal{X},N,\gamma} \gamma \text{ subject to } \mathcal{R}_F(\mathcal{X}, N, G^{[i-1]}, \gamma) \prec 0.$$
4: Solve the optimisation problem
Switch form **do**
case primal
$$\left(G^{[i]}, \gamma^{[i]}\right) = \arg\min_{G,\gamma} \gamma \text{ subject to } \mathcal{R}_p(\mathcal{X}^{[i]}, G, \gamma) \prec 0.$$
case Finsler's
$$\left(\cdot, G^{[i]}, \gamma^{[i]}\right) = \arg\min_{\mathcal{X},G,\gamma} \gamma \text{ subject to } \mathcal{R}_F(\mathcal{X}, N^{[i]}, G, \gamma) \prec 0.$$
5: Update $i = i + 1$.
6: **end**

Output: Matrix $G = G^{[i-1]}$ and scalar $\gamma = \gamma^{[i-1]}$.

Algorithm 1 allows switching when it can no longer reduce γ in either the primal or the Finsler's form. For example, suppose that Algorithm 1 is run in primal (Finsler's) form and returns γ_I and $G_I \in \mathcal{G}_{\gamma_I}$. Then, G_I, γ_I can be used as a starting point for Algorithm 1 in Finler's (primal) form. Such switching is possible because the constraints in the primal and the Finsler's forms are equivalent. The resulting novel algorithm is formalised in Algorithm 2.

Although formal convergence proofs for generic CDAs do not yet exist, CDAs work well in practice and guarantee a non-increasing sequence of γ over the iterations [20]. The study in [18] shows that Algorithm 2 can potentially avoid getting stuck prematurely. Furthermore, the switching nature of Algorithm 2 provides numerical robustness, which is particularly relevant for high-dimensional matrix inequalities and a large number of decision variables.These observations are highlighted in the case studies presented in the next section.

IV. Numerical case studies

This section first presents a realistic case study in Section IV-A. Then, we provide an LTI example in Section IV-B to highlight the numerical properties of Algorithm 2. The source code for both case studies can be downloaded from `https:`

Algorithm 2 Combination of CDAs

Input: Constraints $\mathcal{R}_p \prec 0$ in (23) and $\mathcal{R}_F \prec 0$ in (24), any $\gamma^{[0]} > 0$ and $G^{[0]} \in \mathcal{G}_{\gamma^{[0]}}$, and accuracy threshold $\epsilon > 0$.

1: Set iteration index $k = 1$ and $G_{II}^0 = G^{[0]}$.
2: **while** $(\gamma^{[k-1]} - \gamma^{[k]})/\gamma^{[k]} \geq \epsilon$, **do**
3: Obtain $G_I^{[k]} = G$ and $\gamma^{[k]} = \gamma$ by running Algorithm 1 in primal form starting from $G_{II}^{[k-1]}$.
4: Update $k = k + 1$.
5: Obtain $G_{II}^{[k]} = G$ and $\gamma^{[k]} = \gamma$ by running Algorithm 1 in Finsler's form starting from $G_I^{[k-1]}$.
6: Update $k = k + 1$.
7: **end**

Output: Matrix $G = G_{II}^{[k-1]}$ and scalar $\gamma = \gamma^{[k-1]}$.

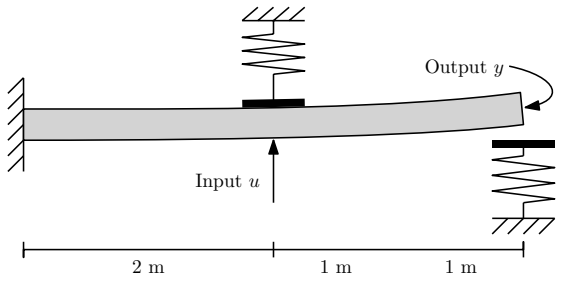

Fig. 2: One-sided clamped flexible beam supported by two nonlinear one-sided springs.

//github.com/FahimShakib. All computations are performed on an Intel Xeon E5-1650, 3.50 GHz processor.

A. Flexible beam with nonlinear support

Consider the flexible beam depicted schematically in Fig. 2. The beam has dimensions of length × width × height = 2 m × 50 mm × 30 mm and is characterised by a Young's modulus of 200 GPa and a density of 7746 kg/m^3. Its dynamics are described by a $n = 48$-dimensional LTI model obtained by the finite-element method. The scalar input u acts in the centre of the beam, while the scalar output y is the deflection at the end of the beam. The $q = 2$ outputs z are the deflections at the locations of the one-sided nonlinear springs, as in Fig. 2. The spring functions can be written as $w = \varphi(z) := 3 \cdot 10^3 \max(0_{2\times 1}, z), z \in \mathbb{R}^2$, where max is an element-wise operator. After a loop transformation [19], the model satisfies all conditions of Theorem 1.

We select the interpolation frequencies $s_1 = 0, s_{2,3} = \pm j \cdot 2\pi 10.2$, and $s_{4,5} = \pm j \cdot 2\pi 64.1$ rad/sec, which correspond to the zero frequency and the frequencies of the first two resonances. We define S and L in (4) as

$$S = \text{blkdiag}\left(0, 2\pi \begin{bmatrix} 0 & 10.2 \\ -10.2 & 0 \end{bmatrix}, 2\pi \begin{bmatrix} 0 & 64.1 \\ -64.1 & 0 \end{bmatrix}\right),$$
$$L = \begin{bmatrix} \ell & \ell & 0_{3,1} & \ell & 0_{3,1} \end{bmatrix}, \quad \ell := \begin{bmatrix} 1 & 1 & 1 \end{bmatrix}^\top.$$

Launching Algorithm 2 from the pair $(G^{[0]}, \gamma^{[0]} = 1.363)$ found by Lemma 3 results in $\gamma = 0.155$. This γ is close to the theoretical lower bound $\gamma > 0.0284$ given by Theorem 3. The lower bound is conservative since it does not take into account moment-matching constraints. In the remainder, the superscript $(\cdot)^\circ$ is used for variables attributed to the initial reduced-order model corresponding to $G^{[0]}$, while variables attributed to the final model are denoted by a hat symbol.

TABLE I: Analysis of the reduction performance in terms of γ (second column), the norms $\|\bar{y}_u\|_2$, $\|\bar{y}_u - \bar{\psi}_u^\circ\|_2$, and $\|\bar{y}_u - \bar{\psi}_u\|_2$ for the block-wave input (third column for the 0.5 Hz input and fourth column for the 10 Hz input), the error bound (12) (fifth column), and the elapsed time for the simulation with input frequency 0.5 Hz, averaged over 5 simulations (last column). The error bound (12) has the same value for both input frequencies.

	γ	0.5 Hz	10 Hz	Error bound	Time [s]
Σ	–	0.132	1.06	–	17.53
$\hat{\Sigma}^\circ$	1.363	0.111	1.591	$3.5 \cdot 10^6$	0.75
$\hat{\Sigma}$	0.155	0.028	0.171	$6.2 \cdot 10^3$	0.46

The Bode magnitude plots of the error between Σ_{lin} and the reduced-order models $\hat{\Sigma}_{lin}^\circ$ and $\hat{\Sigma}_{lin}$ are depicted in Fig. 3. It can be observed that the model $\hat{\Sigma}_{lin}$ (blue curve) obtains a significantly smaller error than the initial model $\hat{\Sigma}_{lin}^\circ$ (red curve), especially for frequencies below 100 Hz. Fig. 4 depicts the steady-state response of the Lur'e-type models $\Sigma, \hat{\Sigma}^\circ$, and $\hat{\Sigma}$ for block-wave excitations with amplitude 10^4 and frequencies $f = 0.5$ Hz and $f = 10$ Hz. The bottom plot shows that the error is significantly reduced, which can also be deduced from Table I. The value of the error bound (12) in Table I also indicates a steep reduction, although the bound is conservative due to approximation steps in its derivation, see [13]. Nevertheless, this study shows that a reduction in the error bound also leads to a reduction in the mismatch between the steady-state responses. The elapsed time for computing the steady-state outputs of $\Sigma_{lin}, \Sigma_{lin}^\circ$, and $\hat{\Sigma}_{lin}$ in Table I shows a significant reduction of over 95%, which is one of the main motivations for model reduction. Solving Problem 1 took less than 30 minutes and successfully reduced a 48-th-order model to a 5-th-order model.

B. Robustness of Algorithm 2 for reducing LTI models

The results of this paper apply to LTI models by neglecting the nonlinearity φ in the models (2) and (7) and taking $q = 0$. Stability preservation is guaranteed by the constraint $\mathcal{N}_\gamma(\mathcal{A}, \mathcal{B}, \mathcal{C}, \mathcal{X}_1) \prec 0$ in $\mathcal{G}_\gamma$ in (20). Therefore, the constraint $\mathcal{N}(S - GL, G_\lambda, H_\zeta, \mathcal{X}_2) \prec 0$ in $\mathcal{G}_\gamma$ can be neglected.

Consider the sixth-order transfer function

$$\Phi(s) = \frac{(s-5)(s-4)(s-3)(s-2)(s-1)}{(s+6)(s+5)(s+4)(s+3)(s+2)(s+1)}, s \in \mathbb{C},$$

and take a minimal, balanced realisation. We reduce this model to a second-order model using Theorem 2 with

$$S = \begin{bmatrix} 0 & 2\pi \\ -2\pi & 0 \end{bmatrix}, \quad L = \begin{bmatrix} 1 & 0 \end{bmatrix}.$$

This results in a family of models parameterised by $G \in \mathbb{R}^2$ and constrained to $\sigma(S) \cap \sigma(S - GL) = \emptyset$. To find the optimal G, we run Algorithm 2 starting from the following

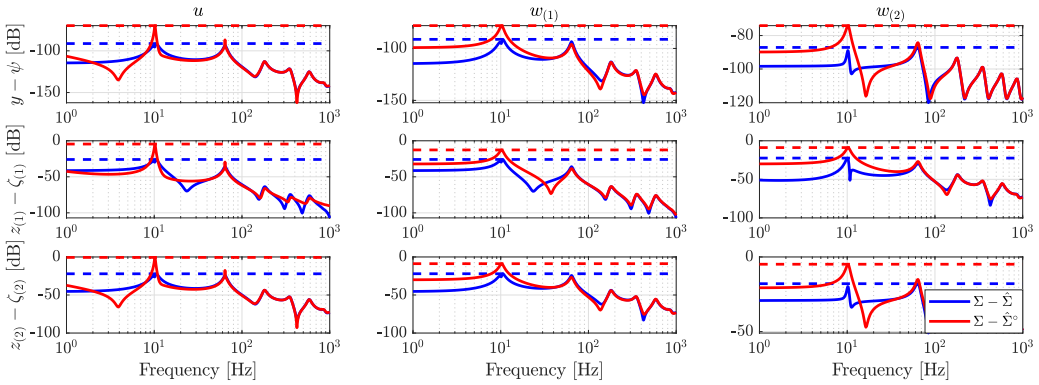

Fig. 3: Bode magnitude plot of error dynamics $\Sigma_{lin} - \hat{\Sigma}^{\circ}_{lin}$ (red) and the error dynamics $\Sigma_{lin} - \hat{\Sigma}_{lin}$ (blue). The horizontal dashed lines indicate the peak error in the correspondingly coloured transfer function.

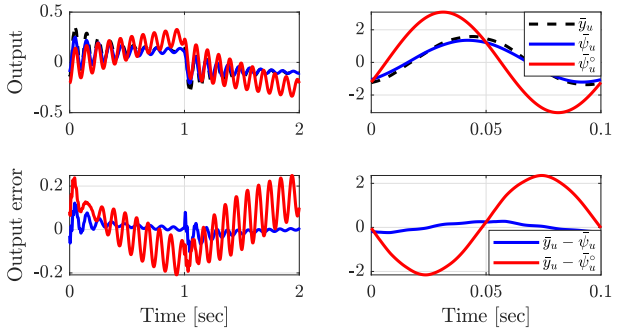

Fig. 4: Top plots: One period of the steady-state output response of the full-order model Σ (black), the initial reduced-order model $\hat{\Sigma}^{\circ}$ (red), and the final reduced-order model $\hat{\Sigma}$ (blue). The input is a block-wave signal with a frequency of 0.5 Hz in the left plots and a frequency of 10 Hz in the right plots. Bottom: The corresponding steady-state error between the outputs of the full-order and reduced-order models.

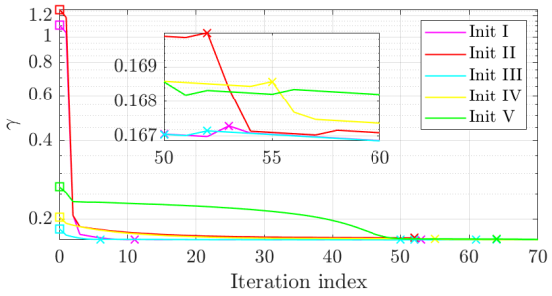

Fig. 5: The iteration history of γ for the starting points in (26). The crosses indicate a switch in Algorithm 2 between the primal and Finsler's form.

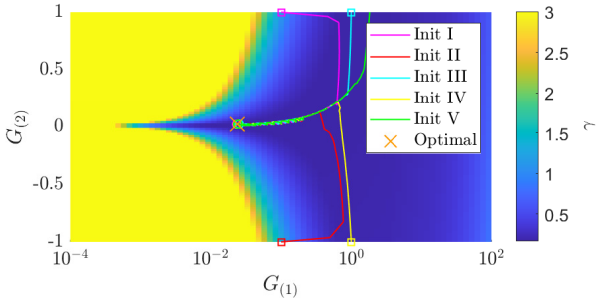

Fig. 6: The colormap of γ over the iteration history of G for the starting points in (26), indicated by the squares, and the final points, indicated by the circles. All curves converge to the same optimal value indicated by the orange cross. For clarity of visualisation, any $\gamma > 3$ is capped at 3.

different initialisations:

$$G^{[0]} = \left\{ \begin{bmatrix} 0.1 \\ 0.1 \end{bmatrix}, \begin{bmatrix} 0.1 \\ -1 \end{bmatrix}, \begin{bmatrix} 1 \\ 1 \end{bmatrix}, \begin{bmatrix} 1 \\ -1 \end{bmatrix}, \begin{bmatrix} 10 \\ 25 \end{bmatrix} \right\}, \qquad (26)$$

called Init I, ..., Init V, respectively. According to Theorem 3, a conservative lower bound for γ is 0.151.

The iteration history in Fig. 5 depicts that, regardless of the starting point, the algorithm converges to approximately the same value of $\gamma \approx 0.166$, which is close to the theoretical conservative lower bound. It also shows that switching, indicated by the cross in Fig. 5, allows γ to be further reduced. Fig. 6 depicts the iteration history of G and shows that G converges to approximately the same solution indicated by the circles, again independent of the starting point indicated by the squares. Crucially, all initialisation result in a G that is close to the optimal G indicated by the orange cross, which was found as a numerical minimiser on a finite grid. We conclude that, in this example, Algorithm 2 is robust to the starting point, since it converges to approximately the same solution regardless of the starting point.Each problem was solved within a few minutes. As can be seen in Fig. 5, the computation time can be significantly reduced by terminating the algorithm prematurely as most of the accuracy improvement occurs in the first few iterations.

V. Conclusions

This paper presents a model reduction approach based on time-domain moment matching for MIMO Lur'e-type models consisting of a feedback interconnection of LTI dynamics and nonlinear static functions. The approach exploits parametric

freedom to minimize the $\mathcal{H}_\infty$-norm of the error transfer-function matrix of the LTI dynamics, which also implies the minimisation of an $\mathcal{L}_2$-error bound on the nonlinear steady-state model responses. Furthermore, both the model structure and the global convergence stability properties of the full-order nonlinear model are preserved.

APPENDIX I
PROOF OF THEOREM 1

Proof: By [22, Theorem 12], model (2) is globally uniformly convergent for the class of inputs $\mathcal{L}_\infty^m$ if, for any input $u \in \mathcal{L}_\infty^m$, (i) there exists a positively invariant compact set with respect to model (2); (ii) model (2) is globally incrementally stable [22, Theorem 12]; and (iii) the vector field is locally Lipschitz in x. The latter condition is satisfied thanks to the incremental sector condition (3). Input-to-state convergence follows from global uniform convergence and input-to-state stability of model (2), see [17].

We first prove the existence of a positively invariant compact set. Consider the function $V = |x|_P^2$, where $|x|_P^2 \coloneqq x^\top P x$ and consider its time-derivative along trajectories of (2):

$$\dot{V} = x^\top (A^\top P + PA)x + 2u^\top B_u^\top P x + 2w^\top B_w^\top P x. \quad (27)$$

Using Young's inequality for products, for any $\gamma_u > 0$, the following inequality holds

$$\begin{aligned} \dot{V} \leq\ & x^\top (A^\top P + PA)x + \frac{1}{\gamma_u}|x|_P^2 + \gamma_u |B_u u|_P^2 \\ & + x^\top P B_w B_w^\top P x + w^\top w. \end{aligned} \quad (28)$$

Furthermore, by the sector condition (3) and $\varphi(0) = 0$, i.e., $w^\top w \leq z^\top z$, we write

$$\begin{aligned} \dot{V} \leq\ & x^\top (A^\top P + PA + P B_w B_w^\top P + C_z^\top C_z)x \\ & + \frac{1}{\gamma_u}|x|_P^2 + \gamma_u |B_u u|_P^2. \end{aligned} \quad (29)$$

Note that by the Bounded-Real Lemma [23], the small-gain condition (6) and A being Hurwitz is equivalent to the existence of a $P \succ 0$ such that $\mathcal{N}(A, B_w, C_z, P) \prec 0$ is satisfied. This implies that, under the condition of Theorem 1, there exists an $\epsilon > 0$ such that

$$A^\top P + PA + P B_w B_w^\top P + C_z^\top C_z \prec -\epsilon P. \quad (30)$$

By (30) and taking $\gamma_u \coloneqq 2\epsilon^{-1}$, it follows from (29) that the following inequality holds:

$$\dot{V} \leq -\frac{\epsilon}{2} V + C_u, \quad C_u \coloneqq 2\epsilon^{-1}|B_u u|_P^2. \quad (31)$$

Using the fact that $u \in \mathcal{L}_\infty^m$, the inequality in (31) implies the existence of a positively invariant set [24, Theorem 1].

Next, we prove global incremental stability. Consider the incremental Lyapunov function $\delta V = \delta x^\top P \delta x$, where $\delta x \in \mathbb{R}^n$ is the difference between two states $x^a \in \mathbb{R}^n$ and $x^b \in \mathbb{R}^n$ (i.e., $\delta x = x^a - x^b$) for the same input $u \in \mathcal{L}_\infty^m$ (i.e., $\delta u = 0$). Using the same steps as in (27)–(31), now for $\delta x \in \mathbb{R}^n$ and $\delta u = 0$, we find that there exists a constant $\epsilon > 0$ such that

$$\dot{\delta V} \leq -\epsilon \delta V \quad \forall\, \delta x \in \mathbb{R}^n. \quad (32)$$

This inequality proves global incremental stability, see [25, Theorem 1]. By the existence of a positively invariant compact set concluded from (31) and global incremental stability concluded from (32), model (2) is globally uniformly convergent by [22, Theorem 12].

Finally, we conclude input-to-state stability of model (2) from the inequality in (31), see [19, Theorem 4.19]. Global uniform convergence and input-to-state stability together imply input-to-state convergence of model (2), see [17].

■

APPENDIX II
PROOF OF LEMMA 1

Proof: The exponentially stable linear dynamics (2a) defines four linear steady-state operators, namely $\mathcal{P}_{(i,k)}, i \in \{y, z\}, k \in \{u, w\}$. Each steady-state operator $\mathcal{P}_{(i,k)}$ defines a mapping from inputs $u \in \mathcal{L}_2^m(T)$ or $w \in \mathcal{L}_2^q(T)$ to the steady-state outputs $\bar{y} \in \mathcal{L}_2^p(T)$ or $\bar{z} \in \mathcal{L}_2^q(T)$. The operator $\mathcal{P}_{(y,u)}$ is incrementally bounded as follows:

$$\left\|\mathcal{P}_{(y,u)}(u_2) - \mathcal{P}_{(y,u)}(u_1)\right\|_2 \leq \gamma_{yu} \left\|u_2 - u_1\right\|_2, \quad (33)$$

where γ_{yu} is defined in accordance with (9). Similarly, all operators $\mathcal{P}_{(i,k)}, i \in \{y, z\}, k \in \{u, w\}$, are bounded using the corresponding constants γ_{ik} in (9). In the same manner, the exponentially stable linear dynamics (7a) of the reduced-order model defines the operators $\mathcal{P}_{(i,k)}, i \in \{\psi, \zeta\}, k \in \{u, \lambda\}$. These operators are also bounded in the sense of (33) with the corresponding constants defined in (9). Furthermore, the inequality

$$\left\|\mathcal{P}_{(i,k)}(\cdot) - \mathcal{P}_{(\hat{i},\hat{k})}(\cdot)\right\|_2 \leq \gamma \left\|\cdot\right\|_2 \quad (34)$$

with γ defined in (11), holds true for all pairs

$$\begin{aligned} (i,k,\hat{i},\hat{k}) \in \{&(y,u,\psi,u), (y,w,\psi,\lambda), \\ &(z,u,\zeta,u), (z,w,\zeta,\lambda)\}. \end{aligned} \quad (35)$$

The mismatch characterised by γ thus bounds the mismatch between the linear operators of the full-order model and the reduced-order model.

Let us consider the mismatch

$$\begin{aligned} \left\|\bar{y} - \bar{\psi}\right\|_2 &= \left\|\mathcal{P}_{(y,u)}(u) - \mathcal{P}_{(\psi,u)}(u) + \right. \\ &\qquad \left. \mathcal{P}_{(y,w)}(\bar{w}) - \mathcal{P}_{(\psi,\lambda)}(\bar{\lambda})\right\|_2 && (36a) \\ &= \left\|\mathcal{P}_{(y,u)}(u) - \mathcal{P}_{(\psi,u)}(u) + \right. \\ &\qquad \mathcal{P}_{(y,w)}(\bar{w}) - \mathcal{P}_{(\psi,\lambda)}(\bar{\lambda}) + \\ &\qquad \left. \mathcal{P}_{(y,w)}(\bar{\lambda}) - \mathcal{P}_{(y,w)}(\bar{\lambda})\right\|_2 && (36b) \\ &\leq \left\|\mathcal{P}_{(y,u)}(u) - \mathcal{P}_{(\psi,u)}(u)\right\|_2 + \\ &\qquad \left\|\mathcal{P}_{(y,w)}(\bar{w}) - \mathcal{P}_{(y,w)}(\bar{\lambda})\right\|_2 + \\ &\qquad \left\|\mathcal{P}_{(y,w)}(\bar{\lambda}) - \mathcal{P}_{(\psi,\lambda)}(\bar{\lambda})\right\|_2 && (36c) \end{aligned}$$

The first and third terms in (36c) can be bounded by (34), and the second term in (36c) can be bounded by (33), resulting in

$$\left\|\bar{y} - \bar{\psi}\right\|_2 \leq \gamma \left\|u\right\|_2 + \gamma_{yw} \left\|\bar{w} - \bar{\lambda}\right\|_2 + \gamma \left\|\bar{\lambda}\right\|_2. \quad (37)$$

Furthermore, (3) implies $\left\|\bar{w} - \bar{\lambda}\right\|_2 \leq \left\|\bar{z} - \bar{\zeta}\right\|_2$, leading to

$$\left\|\bar{y} - \bar{\psi}\right\|_2 \leq \gamma \left\|u\right\|_2 + \gamma_{yw} \left\|\bar{z} - \bar{\zeta}\right\|_2 + \gamma \left\|\bar{\lambda}\right\|_2. \quad (38)$$

Repeating (36)–(38) for the mismatch $\left\|\bar{z}-\bar{\zeta}\right\|_2$, we find

$$\left\|\bar{z}-\bar{\zeta}\right\|_2 \leq \gamma \left\|u\right\|_2 + \gamma_{zw}\left\|\bar{z}-\bar{\zeta}\right\|_2 + \gamma\left\|\bar{\lambda}\right\|_2. \tag{39}$$

From here, we find

$$\left\|\bar{z}-\bar{\zeta}\right\|_2 \leq \frac{\gamma}{1-\gamma_{zw}}\left(\left\|u\right\|_2 + \left\|\bar{\lambda}\right\|_2\right), \tag{40}$$

where the fraction is well-defined since $\gamma_{zw} < 1$ by the gain condition in Theorem 1 under Assumption 1.

Next, we derive a bound for $\left\|\bar{\lambda}\right\|_2$. Note that $\left\|\bar{\lambda}\right\|_2 = \left\|\varphi(\bar{\zeta})\right\|_2 \leq \left\|\bar{\zeta}\right\|_2$ by (3). Furthermore, we have $\left\|\bar{\zeta}\right\|_2 = \left\|\mathcal{P}_{(\zeta,u)}(u) + \mathcal{P}_{(\zeta,\lambda)}(\bar{\lambda})\right\|_2 \leq \left\|\mathcal{P}_{(\zeta,u)}(u)\right\|_2 + \left\|\mathcal{P}_{(\zeta,\lambda)}(\bar{\lambda})\right\|_2$. Then, by (33), we find

$$\left\|\bar{\lambda}\right\|_2 \leq \gamma_{\zeta u}\left\|u\right\|_2 + \gamma_{\zeta\lambda}\left\|\bar{\lambda}\right\|_2, \tag{41a}$$

$$\Rightarrow \left\|\bar{\lambda}\right\|_2 \leq \frac{\gamma_{\zeta u}}{1-\gamma_{\zeta\lambda}}\left\|u\right\|_2, \tag{41b}$$

where the fraction is well-defined since $\gamma_{\zeta\lambda} < 1$ by the gain condition in Theorem 1.

By substituting the bound (41b) for $\left\|\bar{\lambda}\right\|_2$ in (40), we find

$$\left\|\bar{z}-\bar{\zeta}\right\|_2 \leq \frac{\gamma}{1-\gamma_{zw}}\left(1+\frac{\gamma_{\zeta u}}{1-\gamma_{\zeta\lambda}}\right)\left\|u\right\|_2. \tag{42}$$

Finally, substituting the bounds (41b) for $\left\|\bar{\lambda}\right\|_2$ and (42) for $\left\|\bar{z}-\bar{\zeta}\right\|_2$ into (38) and collecting terms, we find the bound (12), which completes the proof. ∎

Appendix III
Proof of Lemma 2

Proof: Consider (7a) and apply the similarity transformation $\xi = \hat{\Theta}^{-1}\hat{\xi}$:

$$\dot{\hat{\xi}} = \hat{\Theta}F\hat{\Theta}^{-1}\hat{\xi} + \hat{\Theta}G\begin{bmatrix}u\\ \lambda\end{bmatrix}, \tag{43a}$$

$$\begin{bmatrix}\psi\\ \zeta\end{bmatrix} = H\hat{\Theta}^{-1}\hat{\xi}. \tag{43b}$$

By (16), we have

$$\dot{\hat{\xi}} = \hat{\Theta}(S-GL)\hat{\Theta}^{-1}\hat{\xi} + \hat{\Theta}G\begin{bmatrix}u\\ \lambda\end{bmatrix}, \tag{44a}$$

$$= \hat{\Theta}S\hat{\Theta}^{-1}\hat{\xi} - \hat{\Theta}GL\hat{\Theta}^{-1}\hat{\xi} + \hat{\Theta}G\begin{bmatrix}u\\ \lambda\end{bmatrix}, \tag{44b}$$

$$\begin{bmatrix}\psi\\ \zeta\end{bmatrix} = C\Pi\hat{\Theta}^{-1}\hat{\xi}. \tag{44c}$$

Now, using (18) and $\hat{\Theta}G = \hat{G}$, we find

$$\dot{\hat{\xi}} = (\hat{F}\hat{\Theta} + \hat{G}L)\hat{\Theta}^{-1}\hat{\xi} - \hat{\Theta}GL\hat{\Theta}^{-1}\hat{\xi} + \hat{\Theta}G\begin{bmatrix}u\\ \lambda\end{bmatrix}, \tag{45a}$$

$$= \hat{F}\hat{\Theta}\hat{\Theta}^{-1}\hat{\xi} + \hat{G}L\hat{\Theta}^{-1}\hat{\xi} - \hat{G}L\hat{\Theta}^{-1}\hat{\xi} + \hat{G}\begin{bmatrix}u\\ \lambda\end{bmatrix}, \tag{45b}$$

$$= \hat{F}\hat{\xi} + \hat{G}\begin{bmatrix}u\\ \lambda\end{bmatrix}, \tag{45c}$$

$$\begin{bmatrix}\psi\\ \zeta\end{bmatrix} = \hat{H}\hat{\Theta}\hat{\Theta}^{-1}\hat{\xi} = \hat{H}\hat{\xi}. \tag{45d}$$

Thus, after performing the similarity transformation and using the specified G, the model is equivalent to (17). To show that $G \in \mathcal{G}_M$, i.e., $\sigma(S)\cap\sigma(S-GL) = \emptyset$, we note that $\sigma(S-GL) = \sigma(\hat{F})$ since a similarity transformation does not affect the eigenvalues. Finally, since $\hat{\Theta}$ in (18) is unique and full rank, we have that $\sigma(\hat{F})\cap\sigma(S) = \emptyset$, and therefore $G \in \mathcal{G}_M$, which completes the proof. ∎

Appendix IV
Proof of Lemma 3

Proof: Since the full-order model satisfies the condition of Theorem 1, there exists a $\tilde{\mathcal{X}} \succ 0$ such that

$$\mathcal{N}(A, B_w, C_z, \tilde{\mathcal{X}}) \prec 0, \quad \tilde{\mathcal{X}} \succ 0_n. \tag{46}$$

Given that $\tilde{\mathcal{X}} \succ 0$ satisfies (46), let us first show that

$$\mathcal{X} = \Pi^\top\tilde{\mathcal{X}}\Pi, \quad G^{[0]} = (\Pi^\top\tilde{\mathcal{X}}\Pi)^{-1}\Pi^\top\tilde{\mathcal{X}}B, \tag{47}$$

satisfy

$$\mathcal{X} \succ 0, \quad \mathcal{N}(S-G^{[0]}L, G_\lambda^{[0]}, C_z\Pi, \mathcal{X}) \prec 0. \tag{48}$$

First, note that $\mathcal{X} \succ 0$ is satisfied since $\Pi \in \mathbb{R}^{n\times\nu}$ is full column rank. The selection (47) gives the identities

$$\mathcal{X}(S-G^{[0]}L) = \Pi^\top\tilde{\mathcal{X}}A\Pi, \quad \mathcal{X}G^{[0]} = \Pi^\top\tilde{\mathcal{X}}B, \tag{49}$$

where the Sylvester equation (13) has been used in the derivation of the first identity. Then, (48) can be manipulated:

$$\mathcal{N}(S-G^{[0]}L, G_\lambda^{[0]}, C_z\Pi, \mathcal{X}) \tag{50a}$$

$$= \mathcal{N}(\mathcal{X}(S-G^{[0]}L), \mathcal{X}G_\lambda^{[0]}, C_z\Pi, I_\nu) \tag{50b}$$

$$= \mathcal{N}(\Pi^\top\tilde{\mathcal{X}}A\Pi, \Pi^\top\tilde{\mathcal{X}}B_w, C_z\Pi, I_\nu) \tag{50c}$$

$$= T^\top\mathcal{N}(\tilde{\mathcal{X}}A, \tilde{\mathcal{X}}B_w, C_z, I_\nu)T \tag{50d}$$

$$= T^\top\mathcal{N}(A, B_w, C_z, \tilde{\mathcal{X}})T \prec 0, \tag{50e}$$

where $T \coloneqq \text{blkdiag}(\Pi, I_{p+m})$. From here, we can conclude that since the matrix T is full column rank, the choice for $\mathcal{X}$ and $G^{[0]}$ in (47) satisfies the inequalities (48). Finally, the change of variables $\begin{bmatrix}Q_1 & Q_2\end{bmatrix} = \mathcal{X}\begin{bmatrix}G_u^{[0]} & G_\lambda^{[0]}\end{bmatrix}$ shows the equivalence between the inequalities (48) and (21), and we can thus conclude that (21) is always feasible, provided that the full-order model satisfies the conditions of Theorem 1.

Satisfaction of (48) results in a $S-G^{[0]}L$ being Hurwitz, which implies asymptotic stability of the linear error dynamics (19). Consequently, there exists an $\mathcal{X}_1 \succ 0$ such that $\gamma^{[0]} = \left\|\Psi-\Gamma\right\|_{\mathcal{H}_\infty} < +\infty$ satisfies $\mathcal{N}_{\gamma^{[0]}}(\mathcal{A}, \mathcal{B}, \mathcal{C}, \mathcal{X}_1) \prec 0$ with $\mathcal{A}, \mathcal{B}$, and $\mathcal{C}$ as in (19). Then, all the constraints in (20) are satisfied and $G^{[0]} \in \mathcal{G}_{\gamma^{[0]}}$, which completes the proof. ∎

Appendix V
Proof of Theorem 3

Proof: We prove the three statements individually.

Statement 1) is proven by noting that the constraints (14b) and (14c) can be written equivalently as the matrix inequality constraints in the set $\mathcal{G}_\gamma$ in (20) by the bounded real lemma [23]. Therefore, $\mathcal{G}_\gamma$ contains all the models that satisfy the constraints (14b) and (14c). To prove that $\mathcal{G}_\gamma$ contains all the models that additionally satisfy the constraint (14d), we first show that $\mathcal{G}_\gamma \subset \mathcal{G}_M$. Under Assumption 1, the

condition $\sigma(S) \cap \sigma(A) = \emptyset$ is satisfied since $\sigma(S) \subset \mathbb{C}^0$, while $\sigma(A) \subset \mathbb{C}^-$. Furthermore, for any $G \in \mathcal{G}_\gamma$, the constraint (14c) ensures that the reduced-order model also satisfies the conditions of Theorem 1 for convergence. Therefore, the condition $\sigma(S) \cap \sigma(S - GL) = \emptyset$ is satisfied for any $G \in \mathcal{G}_\gamma$. Then, by application of Theorem 2 and Lemma 2, the set $\mathcal{G}_\gamma$ contains *all* the models that satisfy the constraint (14d), completing the proof of Statement 1.

Statement 2) contains two statements that are proven separately. First, the set $\mathcal{G}_\gamma$ is non-empty for some $0 \leq \gamma < +\infty$ as a direct consequence of Lemma 3 under Assumption 1. Second, the set $\mathcal{G}_\gamma$ is empty for $\gamma < \bar{h}_{\nu+1}$ by the application of [3, Corollary 1].

Statement 3) is a direct consequence of Lemma 1 after noting that the full model satisfies the conditions of Theorem 1 by assumption and the reduced model satisfies the conditions of Theorem 1 by the constraints in $\mathcal{G}_\gamma$. ■

REFERENCES

[1] A. Antoulas, *Approximation of large-scale dynamical systems*. Philadelphia, USA: SIAM, 2005.

[2] A. Astolfi, "Model reduction by moment matching for linear and nonlinear systems," *IEEE Transactions on Automatic Control*, vol. 55, no. 10, pp. 2321–2336, 2010.

[3] Y. Ebihara and T. Hagiwara, "On $\mathcal{H}_\infty$ model reduction using LMIs," *IEEE Transactions on Automatic Control*, vol. 49, no. 7, pp. 1187–1191, 2004.

[4] S. Gugercin, A. C. Antoulas, and C. Beattie, "$\mathcal{H}_2$ model reduction for large-scale linear dynamical systems," *SIAM journal on matrix analysis and applications*, vol. 30, no. 2, pp. 609–638, 2008.

[5] S. Lagauw, O. M. Agudelo, and B. De Moor, "Globally Optimal SISO H_2-Norm Model Reduction Using Walsh's Theorem," *IEEE Control Systems Letters*, vol. 7, pp. 1670–1675, 2023.

[6] J. M. A. Scherpen, "Balancing for nonlinear systems," *Systems & Control Letters*, vol. 21, no. 2, pp. 143–153, 1993.

[7] A. Sarkar and J. M. A. Scherpen, "Extended differential balancing for nonlinear dynamical systems," *IEEE Control Systems Letters*, vol. 6, pp. 3170–3175, 2022.

[8] A. Padoan, F. Forni, and R. Sepulchre, "Model reduction of dominant feedback systems," *Automatica*, vol. 130, p. 109695, 2021.

[9] B. Besselink, N. van de Wouw, J. M. A. Scherpen, and H. Nijmeijer, "Model reduction for nonlinear systems by incremental balanced truncation," *IEEE Transactions on Automatic Control*, vol. 59, no. 10, pp. 2739–2753, 2014.

[10] B. Besselink, N. van de Wouw, and H. Nijmeijer, "Model reduction for nonlinear systems with incremental gain or passivity properties," *Automatica*, vol. 49, no. 4, pp. 861–872, 2013.

[11] ——, "Model reduction for a class of convergent nonlinear systems," *IEEE Transactions on Automatic Control*, vol. 57, no. 4, pp. 1071–1076, 2011.

[12] M. Zamani and M. Arcak, "Compositional abstraction for networks of control systems: A dissipativity approach," *IEEE Transactions on Control of Network Systems*, vol. 5, no. 3, pp. 1003–1015, 2017.

[13] M. F. Shakib, G. Scarciotti, A. Y. Pogromsky, A. Pavlov, and N. van de Wouw, "Model reduction by moment matching with preservation of global stability for a class of nonlinear models," *Automatica*, vol. 157, p. 111227, 2023.

[14] M. F. Shakib, A. Y. Pogromsky, A. Pavlov, and N. van de Wouw, "Computationally efficient identification of continuous-time Lur'e-type systems with stability guarantees," *Automatica*, vol. 136, p. 110012, 2022.

[15] D. A. Deenen, B. Sharif, S. van den Eijnden, H. Nijmeijer, M. Heemels, and M. Heertjes, "Projection-based integrators for improved motion control: Formalization, well-posedness and stability of hybrid integrator-gain systems," *Automatica*, vol. 133, p. 109830, 2021.

[16] M. F. Shakib, G. Scarciotti, A. Y. Pogromsky, A. Pavlov, and N. van de Wouw, "Time-domain moment matching for multiple-input multiple-output linear time-invariant models," *Automatica*, vol. 152, p. 110935, 2023.

[17] A. Pavlov, N. van de Wouw, and H. Nijmeijer, *Uniform output regulation of nonlinear systems: a convergent dynamics approach*. Boston, USA: Springer Science & Business Media, Birkhäuser, 2006.

[18] M. F. Shakib, G. Scarciotti, M. Jungers, A. Pogromsky, A. Pavlov, and N. van de Wouw, "Optimal $\mathcal{H}_\infty$ LMI-Based Model Reduction by Moment Matching for Linear Time-Invariant Models," in *Proceedings of the 60th Conference on Decision and Control*, 2021, pp. 6914–6919.

[19] H. K. Khalil, *Nonlinear systems*. New Jersey, USA: Prentice-Hall, 1996.

[20] E. Simon, P. R-Ayerbe, C. Stoica, D. Dumur, and V. Wertz, "LMIs-based coordinate descent method for solving BMIs in control design," *IFAC Proceedings Volumes*, vol. 44, no. 1, pp. 10 180–10 186, 2011.

[21] S. Boyd, L. El Ghaoui, E. Feron, and V. Balakrishnan, *Linear Matrix Inequalities in System and Control Theory*, ser. Studies in Applied Mathematics. Philadelphia, PA: SIAM, Jun. 1994, vol. 15.

[22] B. S. Rüffer, N. van de Wouw, and M. Mueller, "Convergent systems vs. incremental stability," *Systems & Control Letters*, vol. 62, no. 3, pp. 277–285, 2013.

[23] C. Scherer, "The Riccati inequality and state-space $\mathcal{H}_\infty$-optimal control." Ph.D. dissertation, Universitat Wurzburg, Germany, 1990.

[24] A. Pavlov, A. Pogromsky, N. van de Wouw, and H. Nijmeijer, "Convergent dynamics, a tribute to Boris Pavlovich Demidovich," *Systems & Control Letters*, vol. 52, no. 3, pp. 257 – 261, 2004.

[25] D. Angeli, "A Lyapunov approach to incremental stability properties," *IEEE Transactions on Automatic Control*, vol. 47, no. 3, pp. 410–421, 2002.